Electronic Supplementary Material (ESI) for Journal of Materials Chemistry B.

Supporting Information

Controlled Free Radical Generation against Tumor Cells by PH-responsive Mesoporous Silica Nanocomposite

Jingke Fu, Yingchun Zhu* and Yang Zhao

Key Lab of Inorganic Coating Materials, Shanghai Institute of Ceramics, Chinese Academy of Sciences, Shanghai 200050, China.

* To whom correspondence should be addressed: Tel.: 86-21-52412632; Fax: 86-21-52412632; E-mail: yzhu@mail.sic.ac.cn.

Supplemental Figures

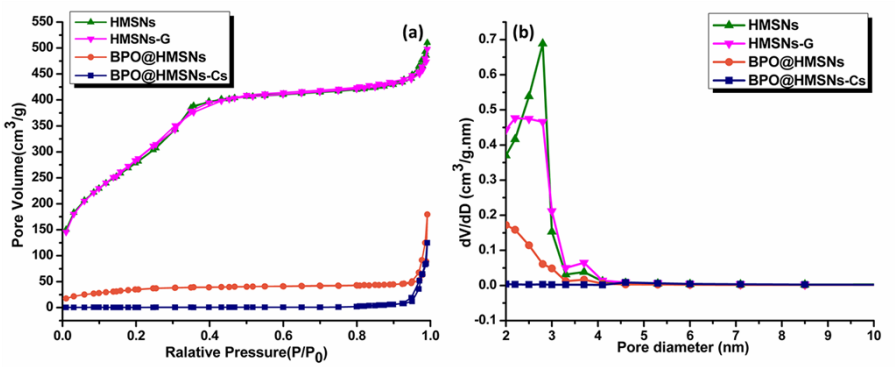

Fig. S1 (a) N_2 adsorption-desorption isotherms of the as-prepared HMSNs, HMSNs-G, BPO@HMSNs and BPO@HMSNs-Cs. (b) The corresponding BJH pore size distribution curves.

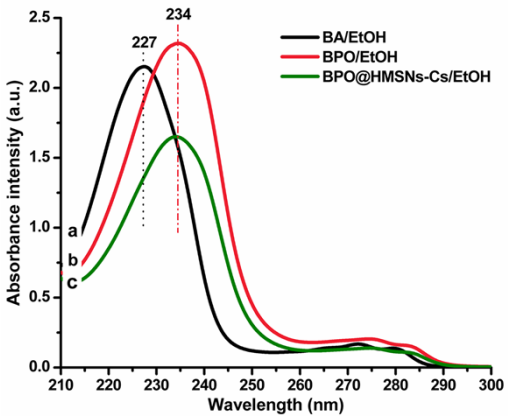

Fig. S2 UV/Vis absorption spectra of (a) BA/EtOH solution, (b) BPO/EtOH solution and (c) BPO@HMSNs-Cs/EtOH solution. The as-prepared BPO@HMSNs-Cs was dispersed in absolute EtOH for 2 h and filtrated through a membrane filter. The obtained filtrate exhibited an absorption peak at 234 nm, which was consistent with the intact BPO in EtOH, demonstrating the integrity of BPO in BPO@HMSNs-Cs.

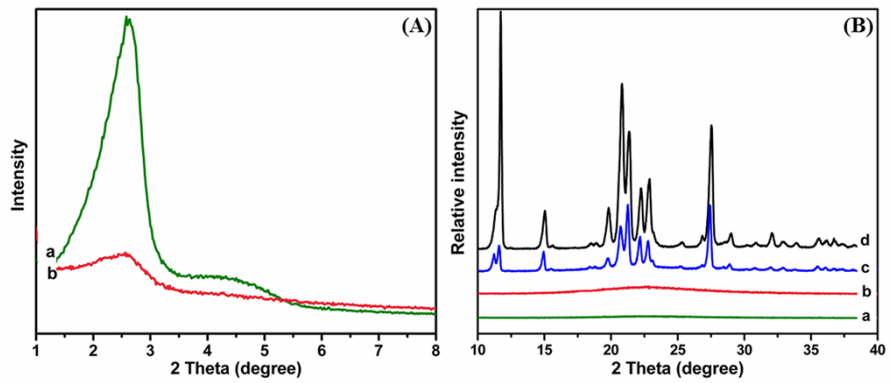

Fig. S3 (A) Small angle XRD patterns of the as-prepared (a) HMSNs and (b) BPO@HMSNs. (B) XRD patterns of (a) HMSNs, (b) BPO@HMSNs, (c) BPO/HMSNs physical mixture and (d) commercial crystalline BPO. The BPO/HMSNs physical mixture showed distinct reflection of crystalline BPO. However, the as-prepared BPO@HMSNs preserved the original matrix structure while showed no peaks attributable to crystalline BPO, demonstrating that the loading procedure inhibited the crystallization of the entrapped BPO molecules in HMSNs.

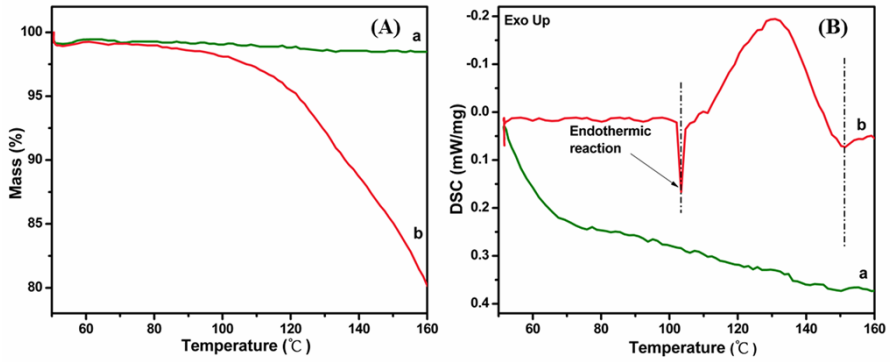

Fig. S4 (A) Thermogravimetry (TG) curves of (a) the as-prepared BPO@HMSNs and (b) crystalline BPO. (B) Differential scanning calorimetry (DSC) curves of (a) the as-prepared BPO@HMSNs and (b) crystalline BPO. The melting of crystalline BPO was clearly visible at 103℃, whereas the as-prepared BPO@HMSNs showed no peaks relative to BPO melting, evidencing that no crystallization of the confined BPO in BPO@HMSNs had occurred.

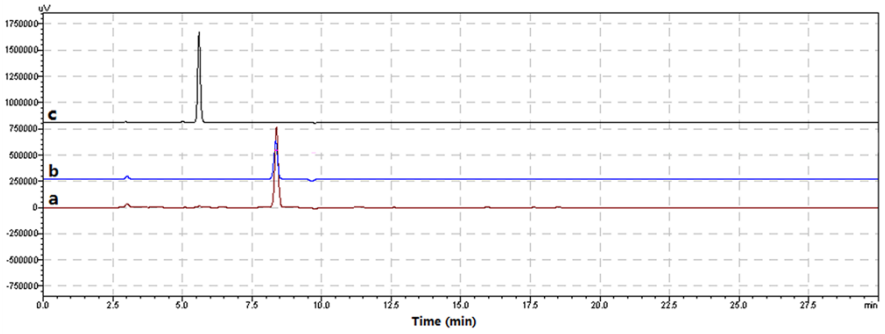

Fig. S5 HPLC of (a) the final release medium, (b) BPO and (c) benzoic acid. The final release medium (at the end of the BPO release from BPO@HMSNs-Cs) was withdrawn and analysed by HPLC to determine the integrity of the released BPO during and after the release process. The HPLC of the final release medium was consistent with that of the intact BPO and no extra peaks relevant to benzoic acid in the chromatogram were detected, demonstrating the preservation of the chemical stability of BPO during and after the release process.

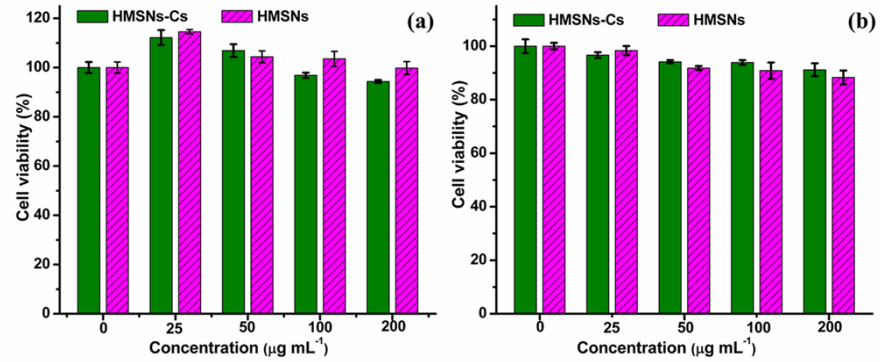

Fig. S6 Viability of ZR75-30 cells exposed to HMSNs or HMSNs-Cs for (a) 24 h and (b) 48 h. Culture media without samples were used as the negative control. The prepared HMSNs and HMSNs-Cs showed high biocompatibility and low toxicity to ZR75-30 cells.

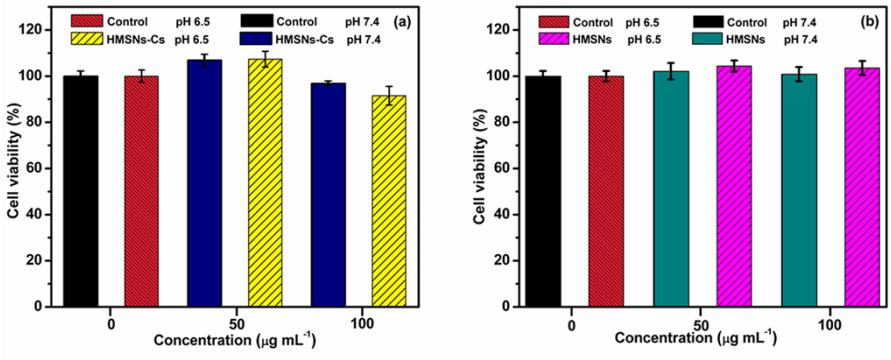

Fig. S7 Cytotoxicity of (a) HMSNs-Cs and (b) HMSNs against ZR75-30 cells after co-incubation for 24 h in pH 7.4 or 6.5 media. Culture media (pH 7.4 and 6.5) without samples were used as the negative controls. Both HMSNs-Cs and HMSNs showed no obvious cytotoxicity difference in culture media of pH 7.4 and 6.5 ($P > 0.05$). Data were represented as means ± SDs (n = 6).

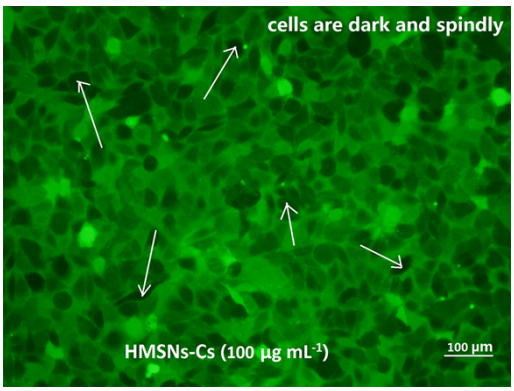

Fig. S8 Fluorescence image of ZR75-30 cells after 4 h exposure to HMSNs-Cs (100 μg mL^{-1}) in serum-free culture media. Negligible green fluorescence was observed in cells (spindly, dark), demonstrating the obtained green fluorescence in cells treated with BPO@HMSNs-Cs (Fig. 8a) was from the oxidizing BPO but not from the HMSNs-Cs carriers.